

The Effect of Stucco Sand Size on the Shell Mould Permeability and Modulus of Rupture (MOR)

Is Prima Nanda,^{a,*}

^{a)} Department of Mechanical Engineering, Faculty of Engineering, Universitas Andalas Padang, 25163 Sumatera Barat, Indonesia

*Corresponding author: isprimananda@yahoo.com

Paper History

Received: 03-January-2018
Received in revised form: 03-February-2018
Accepted: 28-February-2018

ABSTRACT

Investment casting or known as lost wax casting is a technique that offers broad advantages in providing a near-net shaped product and significant to mass production rates. The unique mould making method of IC, able this technique to fulfil complex geometrical shape application. The ceramic shell mould is the key that implies the quality of the product. Permeability and modulus of rupture (MOR) are two dominant properties to be considered. Permeability is important during casting of molten metal to avoid defects or cracks caused by the increased pressure inside due to the blockage of trapped gases to pass throughout the mould. MOR is defined as the strength of the mould to its ability to withstand the stress generated during de-waxing and casting of molten materials. Stucco size is one of the significant factors to affect these subsequent mould properties. In relation to that, this research was conducted to analyse the effect of stucco matrix towards the mould properties. The stucco sand was aluminosilicates formed in two sizes; mesh 50 and mesh 30. The matrix comprises of three types; mesh 50 stuccoed shell mould, mesh 30 stuccoed shell mould, and conjugation of mesh 50 and 30 stuccoed shell mould. The results revealed that the highest permeability of $1.15681 \times 10^{-7} \text{ m}^2$ was obtained from sample B (mesh 50 stuccoed matrix), and peak MOR value of 10.9 MPa was on sample C (mesh 50-30 stuccoed matrix).

KEY WORDS: *Investment casting, permeability, modulus of rupture (MOR), stucco.*

NOMENCLATURE

μ Permeability
 σ Modulus of Rupture

1.0 INTRODUCTION

Investment casting (IC) is one of casting technique that offers broad advantages over the other casting methods [1]. These includes the ability to provide a near-net shape products and variety of casting materials [2,3]. Since the advent of the Second World War, the IC process have been inevitable to modern requirement [4]. IC process comprises of four main procedures; pattern making, shell mould making, casting and post-casting operation. Commonly, for the pattern material, wax is used when mass production needed. Besides that, plastic based material also implemented when prototypes are need to fabricated since the technology of rapid manufacturing (RM) provided significant tools for rapid prototyping (RP) [5]. The ceramic shell mould is built around the pattern by dipping it into a slurry tank containing refractories. Stucco is applied in between the slurry coating to provide strength of the mould, and minimise the drying stress. After the mould have been dried, it will be dewaxed to remove the pattern results in mould cavity for casting. The mould will be fired during the pouring of the molten materials. After solidifies, the mould will be removed and cast product will be further to post-casting operation involves finishing. The ceramic mould is a factor that implies casting quality. The permeability and strength of the mould are significant to affect the casting process, deciding the casting quality [6,7]. Shell mould permeability define as the ability of the mould to pass through gases from the mould cavity inside to the outside during metal pouring [8]. The inefficient permeability will implicate product surface quality in which, the entrapped gases during pouring will repel back to the metal resulting in surface defects. While mould strength, usually quantified as modulus of rupture (MOR), determines the mould ability to withstands shock, density pressure, and handling

operations. Weak mould defined the easiness of cracking to be occurred. Shell mould materials comprises in two categories; slurry and stucco. Slurry is the refractories mixture containing filler and a binder, while stucco is a sand particles and usually aluminosilicates that used due to economic reason [9]. Slurry fillers are very fine in sizes commonly in mesh 200 or 350, while stucco is formed in mesh 50 and 30 sizes. Basically, the approach in constructing the stucco matrix are mesh 50 as the first stucco layers, and mesh 30 for the proceeding coating layers [10]. In relation to that, this research looks at the stucco size matrix manipulation to evaluate its effect on the subsequent properties. By that, the consequence of this study was to reveal better stucco matrix sizes to achieve better mould quality.

2.0 MATERIALS AND METHOD

2.1 Pattern

The pattern used in this research consist of two types, correspond to the parameters to be tested. For permeability test sample, the pattern was a table tennis ball attached to a hollow mullite rod, as shown in Figure 1. While for the modulus of rupture (MOR) test sample, a rectangular wax is used as the pattern as shown in Figure 2. These pattern shaped are common in conducting the correspond parameters [6]. The concept of the permeability test sample using a table tennis ball is due to its spherical geometry that ensure the uniform air distribution inside the mould surface. For the MOR test sample, the intention was to produce a plate, to be used in bending test.

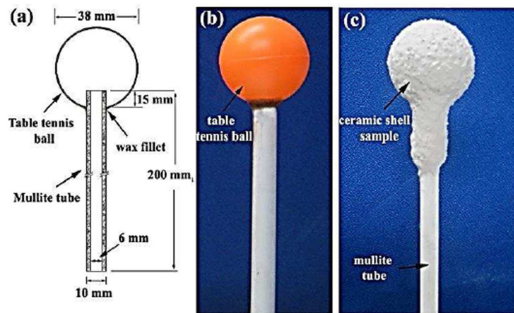


Figure 1: Permeability test sample pattern: (a) schematic illustration of the pattern sample, (b) a typical pattern sample, (c) ceramic coated sample



Figure 2: Modulus of Rupture (MOR) test sample pattern

2.2 Slurry

The slurry developed for this experiment comprises of zircon flour ($ZrSiO_4$) as the refractory filler, with colloidal silica (SiO_2) binder. The stucco sand was aluminosilicates (Al_2SiO_5) formed in two sizes, mesh 50 and 30. The slurry was prepared with two viscosities as shown in Table 1, namely, the primary slurry and secondary. The viscosity of the slurry was measured using Zahn cup #5.

Table 1: Slurry Specification

Slurry Type	Refractory filler	Binder	Viscosity (s)
Primary	Zircon flour	Colloidal	14
Secondary	(200 mesh)	silica	17

2.3 Shell mould

All the prepared pattern samples were coated with ceramic slurry and stuccoed with investigated sizes as shown in Table 2. Sample A described the permeability and MOR test samples that were built with mesh 50 stucco sand size as its stucco matrix. Sample B on the other hand was been stuccoed with mesh 30 aluminosilicates whereas Sample C stucco matrix was a conjugation of mesh 50 and 30. All the test samples were fabricated with specification shown in Table 3. The sample was dipped into the ceramic slurry for 30 second, and then drained about the same period before proceeds to drying. Next, the sample was dipped again into the secondary slurry for building the backup coat, and then stuccoed with investigated mesh sizes with rainfall method. Lastly, a seal coat of secondary slurry was applied and the mould were left to dry for about 48 hours. Total of 7 layers of coating were developed for every shell mould samples. All the samples were dewaxed in an electrical firing furnace for 1 hour in $200^\circ C$ temperature with $20^\circ C/3.4$ min heating rates. The samples were then proceeds to firing in the furnace for $700^\circ C$ in the rate of $11.67^\circ C/min$.

Table 2: Shell Mould Coating Specification for Three Investigated Samples (A, B and C)

Coating level	Slurry type	Stucco matrix		
		Sample A	Sample B	Sample C
Primary	Primary	-	-	-
Backup 1	Secondary	Mesh 50	Mesh 30	Mesh 50
Backup 2	Secondary	Mesh 50	Mesh 30	Mesh 30
Backup 3	Secondary	Mesh 50	Mesh 30	Mesh 50
Backup 4	Secondary	Mesh 50	Mesh 30	Mesh 30
Backup 5	Secondary	Mesh 50	Mesh 30	Mesh 50
Seal	Secondary	-	-	-

Table 3: Shell Mould Building Specification

Coating level	Dip time	Drain time	Dry time
	second	second	hour
Primary	30	30	2
Backup 1	30	30	4
Backup 2	30	30	4
Backup 3	30	30	4
Backup 4	30	30	4
Backup 5	30	30	4
Seal	30	30	48

2.4 Permeability measurement

The permeability values of the samples were determined using the apparatus as shown in Figure 3a and 3b. The permeability test sample was connected with a rubber tube of the permeability test equipment, permitting the pressurizes air to flow through the sample. The pressure of the air was setup to 5 psi or 34.5 kN.m2 at the room temperature of 25°C. The permeability number (μ , m2), is calculated according to BS1902-10.2:1994 standard (determination of permeability and standard air flow capacity at elevated temperature) [11] by measuring of the air flow through the shell mould samples at a given pressure and temperature using Equation 1.

$$\mu = \frac{(\eta)(V_c)(l)}{(a)(P)} \quad (1)$$

where η , is the dynamic air viscosity at the experimented temperature (Ns/m^2), V_c , is the air volumetric flow rate corrected for expansion at higher temperatures (m^3/s), l , is the thickness of shell mould (m), a , is the inner surface value of the hollow shell (m), and P , is the pressure difference across the shell mould (N/m^2).

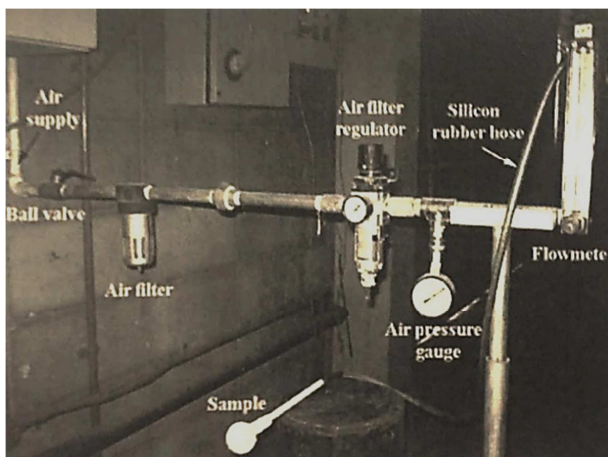


Figure 3a: Permeability test set-up apparatus used to perform permeability measurement of the test samples

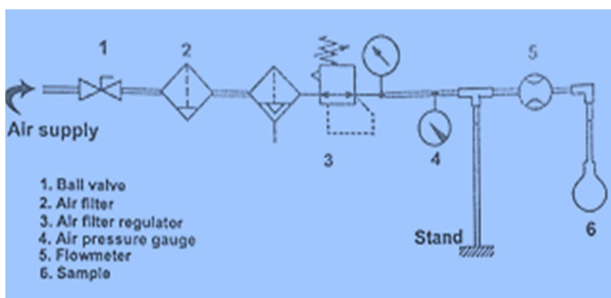


Figure 3b: Schematic diagram of the permeability test apparatus

2.5 Modulus of Rupture (MOR) measurement

The modulus or rupture (MOR) of every samples were measured by performing a 3-points flexural bending strength test using a

Universal Testing Machine as shown in Figure 4. The modulus of rupture (MOR) (σ , MPa) of every shell mould samples were calculated by using Equation 2. From the Universal Testing Machine, the maximum fracture load (P) is obtained.

$$\sigma = \frac{(3)(P)(L)}{(2)(W)(H^2)} \quad (2)$$

where σ is the modulus of rupture (MPa), P is the maximum load applied until fracture occur (N), L is the length of span between two hold point (m), W is the width of the test samples (m), and H is the thickness of the test samples (m). The MOR test samples was 4 mm thick, 10 mm width and the length of span was setup to be 64 mm.

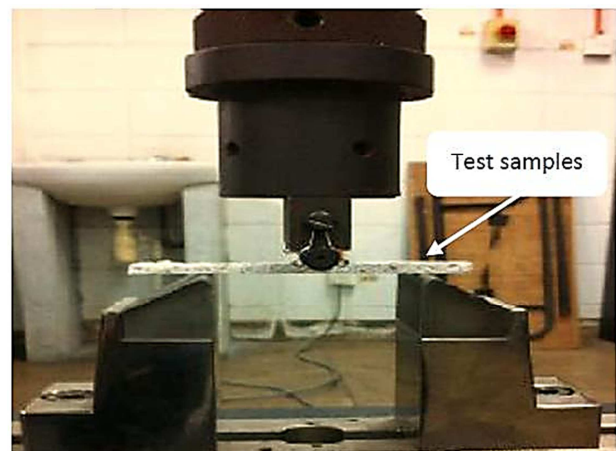


Figure 4: Universal Testing Machine (Model: Instron) used to perform a 3-points flexural bending strength for the Modulus of Rupture (MOR) test samples.

3.0 RESULTS AND DISCUSSION

The results of the permeability and modulus of rupture (MOR) of the investigated sample A, B and C are tabulated in Table 4. The permeability and MOR results are graphically illustrated as Figure 5 and 6, and the microstructures of those test samples are shown in Figure 7 and 8. Based on the results obtained, sample B showed the highest permeability value, compared to sample A and C. While for MOR, sample C was at peak value rather than sample B and A. Sample A was built with stucco size mesh 50 matrix, was the least of both respond parameters. The microstructures of these samples gave a visual understanding of the results. Sample A of both permeability and MOR test samples, having packer and tighter particles arrangement, and also less gaps and holes exhibits. The fine stucco sand responsible for creating the dense particles arrangement. As for sample B, which was constructed with stucco sand of size mesh 30 as its stuccoes matrix, can be seen to have larger crates and gaps, exist on its particles packing. Coarse stucco of sample B provide wider gaps, less dense, and limited particles inter-bonding, in which results in highly porous samples. By that, the porosity of sample B ease the flow of air through the mould sample. Although coarse stucco implies excellent permeability, due to lack of inter-bonding of the

stucco particles, the sample strength was vice versa. On the other hand, sample C, in which was constructed by a conjugation of mesh 50 and 30 stucco as its mould matrix, was revealed to be in median values of both parameters. The permeability of sample C was less than sample B but its strength (MOR) was higher. The microstructures of sample C was seen to be better with no sudden large crates or gaps, in which, the porosity was observed to be more uniformed than sample B. Due to its matrix, the quality of permeability and MOR was generated conveniently. The inter-bonding of sample C particles, was achieved highly with uniform particles arrangement, with more porous than sample A, but less porous than sample B.

Table 4: Permeability Results of Three Shell Mould Samples (A, B and C)

Sample type	Stucco size matrix	Permeability, μ	Modulus of rupture, σ
		m^2	MPa
A	Mesh 50	1.14008×10^{-7}	6.727
B	Mesh 30	1.15681×10^{-7}	9.893
C	Mesh 50-30	1.14715×10^{-7}	10.898

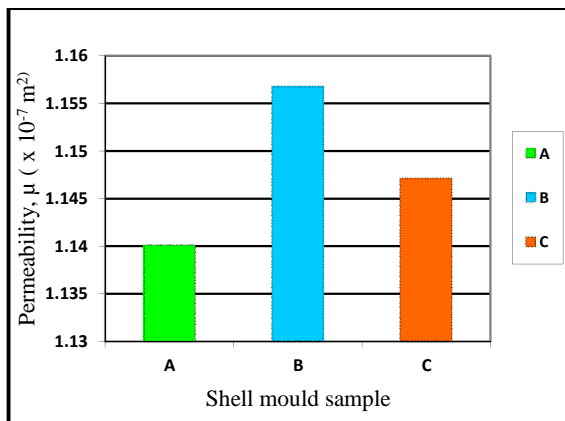


Figure 5: Graph of Permeability Values of Sample A, B and C

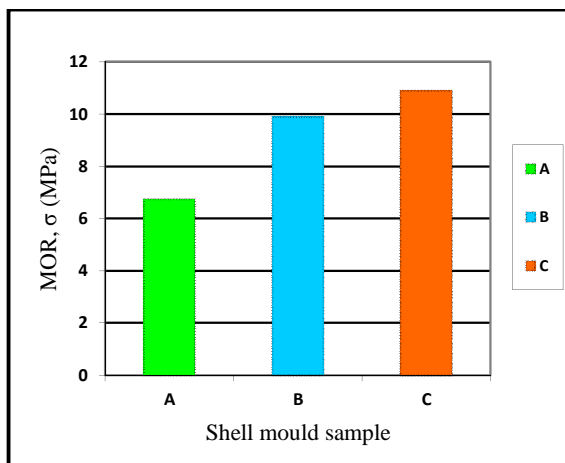


Figure 6: Graph of MOR Values of Sample A, B and C

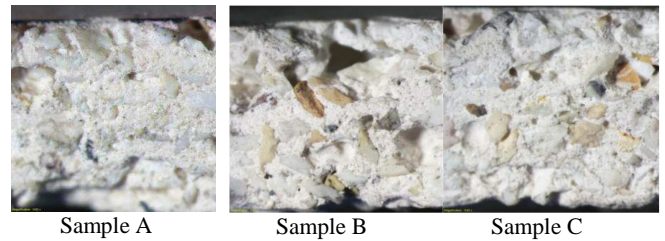


Figure 7: Microstructure of Permeability Test Sample A, B and C

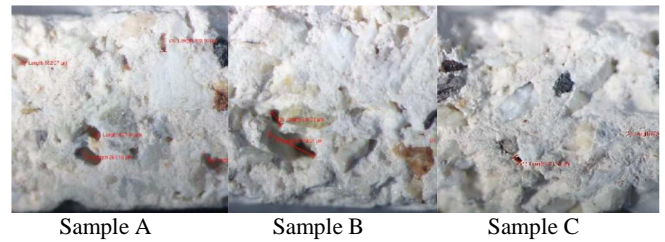


Figure 8: Microstructure of MOR Test Sample A, B and C

4.0 CONCLUSION

The research was conducted to investigate the effect of different stucco matrix towards the shell mould permeability and Modulus of Rupture (MOR). The matrixes were sample A stuccoed with mesh 50 aluminosilicates, sample B stuccoed with mesh 30, and sample C stuccoed with conjugation of mesh 50 and 30. For every sample, permeability and modulus of rupture (MOR) test samples were produced and measured by performing permeability test and 3-points flexural bending strength test. This investigation found that stucco sizes and type of matrix are significant to affect the shell mould permeability and modulus of rupture (MOR). The permeability was highest on sample B ($1.15681 \times 10^{-7} m^2$) followed by sample C ($1.14715 \times 10^{-7} m^2$) and sample A ($1.14008 \times 10^{-7} m^2$). The microstructures of the permeability test samples A, B and C gave an observation of its pores whereas larger pores exhibit by sample B, than sample C and sample A. For the modulus of rupture (MOR), the strongest mould was measured on sample C (10.898 MPa). Sample B (9.893 MPa) was lesser than sample C, but both values were higher than sample A (6.727 MPa). The MOR test samples microstructures was observed and sample C particles was more compacted rather than sample B with large pores and sample A with several small pores. It can be concluded that the manipulation of shell mould stucco matrix defines the mould properties. However, the first layer of stucco should be in fine size which is mesh 50, to prevent the occurring of crack during drying phase [3,12]. The first ceramic coating having low viscosities, and the drying stress can result in cracking of the mould. Thus, the fine stucco sand can be able to cover up all the surfaces of the coating to minimise the drying stress. In relation of that, implementing the stucco matrix as sample C, is more convenience rather than sample B due to drying stress factor. Also, sample C is better approach than sample A in term of permeability of the shell mould. Apart from that, a good recommendation can be attached to improve this area of study is employing Design of Experiment (DOE) method to conduct

experiments for the optimum stucco matrix. Besides that, sample C was mesh 50 for it last stucco layer in this investigation, and thus, the investigation can be prolonged with mesh 30 as the last stucco layer before a seal coat applied.

ACKNOWLEDGEMENTS

The authors would like to convey a great appreciation to the Department of Material, Manufacturing and Industry of Faculty of Mechanical Engineering at Universiti Teknologi Malaysia (UTM) Skudai Johor Malaysia and the Department of Mechanical Engineering, Universitas of Andalas for the financial assistance and used of research facilities. The authors are also indebted to everyone in involving in this research.

REFERENCE

1. M. Rahimian, S. Milenkovic, L. Maestro, A. E. R. De Azua, and I. Sabirov, "Physical Simulation of Investment Casting of Complex Shape Parts," *Metall. Mater. Trans. A Phys. Metall. Mater. Sci.*, vol. 46, no. 5, pp. 2227–2237, 2015.
2. J. Campbell, "The concept of net shape for castings," *Mater. Des.*, vol. 21, no. 4, pp. 373–380, 2000.
3. I. B. Dave and V. . N. Kaila, "Optimization of Ceramic Shell Mold Materials in Investment Casting," *Int. J. Res. Eng. Technol.*, vol. 3, no. 10, pp. 30–33, 2014.
4. R. Prasad, "Progress in Investment Castings," *Sci. Technol. Cast. Process*, pp. 25–72, 2012.
5. S. Singh and R. Singh, "Precision investment casting: A state of art review and future trends," *Proc. Inst. Mech. Eng. Part B J. Eng. Manuf.*, vol. 230, no. october 14, pp. 1–22, 2016.
6. S. Amira, D. Dubé, and R. Tremblay, "Method to determine hot permeability and strength of ceramic shell moulds," *J. Mater. Process. Technol.*, vol. 211, no. 8, pp. 1336–1340, 2011.
7. J. Zych, J. Kolczyk, and T. Snopkiewicz, "New Investigation Method of the Permeability of Ceramic Moulds Applied in the Investment Casting Technology / Nowa metoda oceny przepuszczalności form ceramicznych stosowanych w technologii wytapianych modeli," *Arch. Foundry Eng.*, vol. 13, no. 2, pp. 107–112, 2013.
8. T. Branscomb, "A New Method of Measuring Green and Fired Permeability of Investment Casting Shells," in *52nd Technical Conference & Equipment Expo*, 2004, pp. 1–9.
9. C. Yuan, S. Jones, and S. Blackburn, "Development of a new ferrous aluminosilicate refractory material for investment casting of aluminum alloys," *Metall. Mater. Trans. A Phys. Metall. Mater. Sci.*, vol. 43A, no. 13, pp. 5232–5242, 2012.
10. B. A. Ramachandran M, "Effect of Process Parameters on Roughness and Hardness of Surface and Dimensional Accuracy of Lost Wax Process Casting," *J. Mater. Sci. Eng.*, vol. 4, no. 4, pp. 1–4, 2015.
11. H. Jafari, M. H. Idris, and A. Ourdjini, "Effect of Thickness and Permeability of Ceramic Shell Mould on In Situ Melted AZ91D Investment Casting," *Appl. Mech. Mater.*, vol. 465–466, no. 5, pp. 1087–1092, 2014.
12. P. Kumar, I. S. Ahuja, and R. Singh, "Experimental investigations on hardness of the biomedical implants prepared by hybrid investment casting," *J. Manuf. Process.*, vol. 21, pp. 160–171, 2016.